# Local transverse coupling impedance measurements in a synchrotron light source from turn-by-turn acquisitions

Michele Carlà, Gabriele Benedetti, Thomas Günzel, Ubaldo Iriso, and Zeus Martí
*ALBA-CELLS Synchrotron Radiation Facility, Carrer de la Llum 2-26, 08290—Cerdanyola del Valles, Barcelona, Spain*
(Received 13 June 2016; published 19 December 2016)

Transverse beam coupling impedance is a source of beam instabilities that limits the machine performance in circular accelerators. Several beam based techniques have been used to measure the transverse impedance of an accelerator, usually based on the optics distortion produced by the impedance source itself. Beam position monitor turn-by-turn analysis for impedance characterization has been usually employed in large circumference machines, while synchrotron light sources have mainly used slow orbit based techniques. Instead, the work presented in this paper uses for the first time turn-by-turn data at ALBA to advance the measurement technique into the range of the typically small impedance values of modern light sources. We have measured local impedance contributions through the observation of phase advance versus bunch charge using the betatron oscillations excited with a fast dipole kicker. The ALBA beam position monitor system and the precision of the turn-by-turn analysis allowed to characterize the main sources of transverse impedance, in good agreement with the model values, including the impedance of an in-vacuum undulator.

DOI: 10.1103/PhysRevAccelBeams.19.121002

## I. INTRODUCTION

Transverse coupling impedance plays a steadily growing role in the landscape of synchrotron light sources, where new designs require small sized beam pipes, multilayer materials, and complex vacuum chamber structures. All such elements contribute to the machine impedance budget, whose evaluation is a key task in the design stage of a new machine since the maximum current that can be stored in an accelerator depends on the ring impedance.

A local impedance source produces a small transverse defocusing effect, whose strength depends on the bunch charge and results in a machine optics distortion in the form of an average tune shift or betatron amplitude/phase beat with current [1,2]. Measurements of the average tune shift with current are used to evaluate the global transverse impedance of the machine and have been extensively performed in different accelerators [3–5], including ALBA [6,7]. Global impedance measurements are also a valid tool to evaluate local impedance source using a differential approach provided that the mechanical settings of a particular element in the machine can be changed between two global measurements as in the case of movable devices such as scrapers or in-vacuum undulators (IVU). Unfortunately in the case of IVUs the presence of a magnetic field that changes along with the jaws position makes such tempting approach not practical, requiring a very good magnetic characterization in order to disentangle the effects induced by impedance from the magnetic one.

In this paper, we determine localized impedances around the ALBA ring by fitting the phase beat with current. This technique can be carried out using two main approaches: closed orbit or turn-by-turn beam position measurements.

While the first one has been the choice of reference in light sources like APS or Diamond [8,9], the turn-by-turn method has been mainly applied to larger circumference machines like SPS, RHIC or LHC [10–13]. This work reports on the use of turn-by-turn method for the impedance measurement in a synchrotron light source whose localized impedances are typically at least one order of magnitude smaller than those in the cited hadron and ion rings.

Taking advantage of the turn-by-turn capabilities of the last generation beam position monitors (BPMs), we successfully apply the turn-by-turn technique to estimate the major contributors to the impedance budget of ALBA. Furthermore we found how smaller impedance sources can still be precisely characterized by performing a lattice manipulation that enhances the small effect at the location of an IVU.

In this work, we show how the results of the turn-by-turn measurements agree with the transverse impedance model based on computer simulations: for all elements analyzed in this paper, the discrepancies are within the 10% experimental error, except on one case which shows a 20% deviation. This not only stresses the good performance of the measurement technique, but also the impedance model itself.

We organize this paper as follows. In Sec. II the basics of transverse coupling impedance and transverse beam

dynamics are covered. Section III is dedicated to description of the experimental set-up, while in Sec. IV the results of measurements on the ALBA synchrotron light source are presented. Finally we summarize the results and discuss possible improvements of the presented technique.

## II. TRANSVERSE COUPLING IMPEDANCE AND BETATRON MOTION

### A. Defocusing kick induced by a transverse impedance

The electromagnetic interaction between a charged beam and the vacuum chamber leads to the excitation of a wakefield. Among other effects a small defocusing of the beam is usually induced by the subsequent interaction between particles and the wakefield itself. A detailed analysis of the phenomenon is found in literature [1]. The analytic expression of the equivalent defocusing quadrupole-like kick per unit length, produced by a transverse coupling impedance source $Z^{\mathrm{eff}}_{\mathrm{H,V}}$ on an ultra-relativistic bunch of particles with Gaussian longitudinal profile is

$$\Delta K_{\mathrm{H,V}} = -\frac{N_p q^2}{E_0}\mathrm{Im}(Z^{\mathrm{eff}}_{\mathrm{H,V}})\frac{1}{2\sqrt{\pi}\sigma_\tau}, \tag{1}$$

where $N_p$ is the number of particles populating the bunch, $q$ the charge of each particle, $\sigma_\tau$ is the Gaussian bunch length in time units and the subscripts H, V stand for horizontal or vertical plane.

Note that, for asymmetric structures, the defocusing kick has different strength on the vertical and horizontal planes. This is the case of synchrotron light sources, where an extensive use of flat beam pipes and the presence of many insertion devices can easily lead to a significant effect on the vertical plane, while being negligible on the horizontal one. For this reason only the effect on the vertical plane has been considered in this paper.

### B. Optics observation through turn-by-turn measurements

Given a nominal model for the machine optics, a defocusing kick of integrated strength $\Delta K$ produces a distortion of the horizontal and vertical betatron amplitude $\beta(s)$ and phase $\psi(s)$ of the form [10,14]:

$$\frac{\Delta\beta(s_n)}{\beta^0(s_n)} = -\frac{\beta(s_k)}{2\sin(2\pi Q)}\cos(2|\psi(s_n)-\psi(s_k)|-2\pi Q)\Delta K, \tag{2}$$

$$\Delta\psi(s_n) = \begin{cases} \dfrac{\beta(s_k)\Delta K}{2}\left(1+\dfrac{\cos(2\psi(s_k)-\psi(s_n))\sin(\psi(s_n)-2\pi Q)}{\sin(2\pi Q)}\right) & \text{if } s_n > s_k \\ \dfrac{\beta(s_k)\Delta K}{2}\dfrac{\sin(\psi(s_n)\cos(\psi(s_n)-2\psi(s_k)+2\pi Q)}{\sin(2\pi Q)} & \text{if } s_n \le s_k, \end{cases} \tag{3}$$

where, $s_k$ is the kick position, $s_n$ is the position of an observer (i.e., BPM) and $Q$ is the machine betatron tune. To get rid of the overall betatron phase of the BPMs, we proceed by defining a new quantity $\Delta\psi^\dagger(s_n)$ as the difference of the phase beat observed by two neighbor BPMs:

$$\Delta\psi^\dagger(s_n) = \Delta\psi(s_n) - \Delta\psi(s_{n+1}). \tag{4}$$

Since both quantities, $\frac{\Delta\beta(s_n)}{\beta^0(s_n)}$ and $\Delta\psi^\dagger(s_n)$, behave linearly in presence of small quadrupolar errors, a simple linear regression should be effective to disentangle the effect of multiple and distributed impedance sources given a set of two beta or phase measurements performed at different bunch charge. For this purpose we proceed by creating a simulated response matrix $M$ containing the expected change of the betatron phase and amplitude resulting from a unitary defocusing kick located at each one of the different impedance sources. The pseudo-inverse matrix $M^{-1}$ has been obtained from $M$ by means of singular value decomposition. Given a set of measured beta or phase variations $\Delta\vec{V}$ the strength of each impedance source $\vec{Z}$ is reconstructed as:

$$\vec{Z} = M^{-1}\Delta\vec{V}. \tag{5}$$

## III. ALBA EXPERIMENTAL SETUP

ALBA is a 3 GeV third generation synchrotron light source, whose main parameters are listed in Table I. It is equipped with 6 insertion devices (IDs) of which 3 use flat NEG coated aluminum chambers, 2 are IVUs and one is a superconducting wiggler (SCW). The injection is obtained by means of 4 kickers employing a ceramic vacuum

TABLE I. ALBA storage ring main parameters.

| | |
|---|---|
| Circumference | 268.8 m |
| Revolution Frequency | 1.115 MHz |
| Energy | 3.0 GeV |
| $Q_x$ | 18.155 |
| $Q_y$ | 8.362 |
| Operational Current | 150 mA |
| Operational Bunch Charge | 0.40 nC |
| Operational Bunch Length | 20 ps |

TABLE II. ALBA storage ring vertical impedance budget. Standard beam pipe refers to the overall contribution of the standard vacuum chamber used in most parts of the machine. The IVU value corresponds to the minimum gap (6 mm), while being negligible at full open position. The contribution of the vertical scraper has been characterized for different gaps other than the nominal position at ±4.75 mm, in all cases the jaws aperture was kept symmetric with respect to the beam.

| Element | Impedance [kΩ/m] | Kick [1/(Am)] |
|---|---|---|
| Injection section | 25.3 | 0.098 |
| IVU | 38.2 | 0.147 |
| NEG-coated Al-chamber | 31.2 | 0.120 |
| Superconducting wiggler | 14.6 | 0.056 |
| Standard beam pipe | 105.6 | 0.404 |
| Scraper ± 4.75 mm | 10.6 | 0.041 |
| Scraper ± 3.0 mm | 24.1 | 0.093 |
| Scraper ± 2.5 mm | 38.4 | 0.148 |
| Scraper ± 2.0 mm | 59.5 | 0.230 |

chamber coated with a 0.4 m layer of Titanium [15]. Along with the standard beam pipe, these devices account for most of the total transverse impedance budget.

A further strong source of impedance is provided by the vertical beam scraper located in the injection section. This element is of particular interest for this study: the ability to change its position and so to modulate its impedance contribution, provides a good test-bench to prove the functionality of the measurement setup.

Table II shows the main contributors to the ALBA impedance budget along with the produced defocusing kick obtained from the combination of geometrical and resistive wall transverse impedance, the former computed analytically while the latter with the simulation code GdfidL [16]. The listed values not only correspond to the main structures, but also to the nearby transition elements like absorbers, tapers, etc.

Since the beta and phase beating produced by a defocusing kick are proportional to $\beta(s)$ at the kick location [Eqs. (2)–(3)], the betatron amplitude has to be accounted for when evaluating the impact of different impedance sources. Figure 1 shows the optical functions for the ALBA storage ring along with the positions of the most important impedance sources. The contribution of the low-gap chambers and IVUs used in the straight sections is mitigated by the small value of the average vertical $\bar{\beta} \sim 1.2$ m at their location whereas a larger weight is given to the injection zone and the standard beampipe which are located at higher $\bar{\beta} \sim 6.5$ m.

### A. BPMs and turn-by-turn observations

A fast magnetic kicker [17] along with 120 BPMs equipped with "Libera Brilliance" electronics [18] allowed turn-by-turn observations [19]. The setup of the BPMs resulted to be one of the most critical steps, requiring a great deal of work before it was possible to collect proper turn-by-turn measurements. In fact in order to reach the temporal resolution required to discriminate the beam position on a turn-by-turn basis, it was necessary to replace the slow time constant filter used in the default firmware

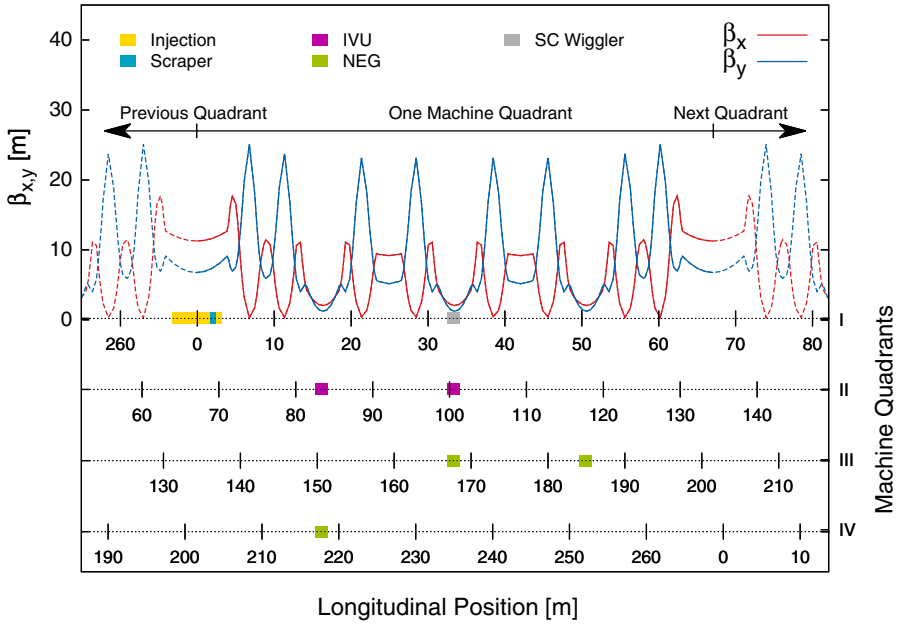


FIG. 1. Betatron functions and location of the major transverse impedance sources in the ALBA storage ring. The ring nominal lattice has a fourfold symmetry, where each quadrant is composed by two Chasman-Green cells surrounded by two matching cells. The injection section is between two matching cells where the vertical betatron function reaches higher values.

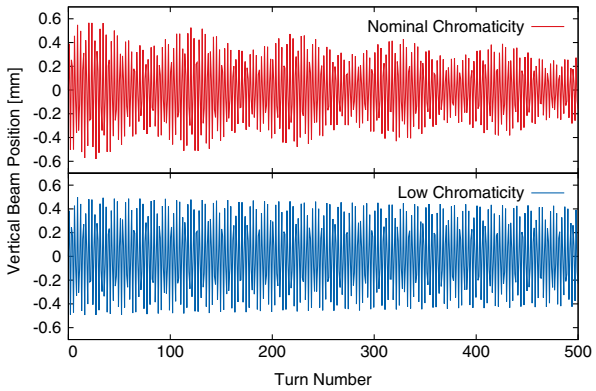


FIG. 2. Turn-by-turn vertical beam position measurements for the standard operation and zero chromaticity lattice. In the standard operation case (upper plot) a fast damping along with the characteristic pulsating amplitude is observed while the zero chromaticity case (lower plot) has an almost purely exponential decay.

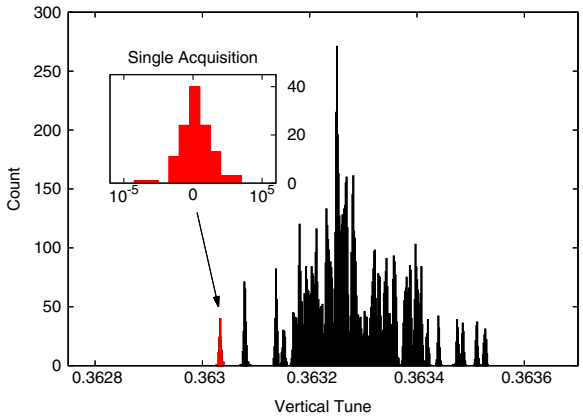


FIG. 3. Histogram of the vertical tune measured by 120 BPMs for 100 acquisitions. The measurement shows an overall standard deviation of $1.1 \times 10^{-4}$, on the other hand looking at one single acquisition (in red) the spread is strongly reduced presenting a standard deviation of only $2.1 \times 10^{-6}$.

with a new one, where a finite impulse response filter of the moving average window type is used [20,21].

The two observables of interest, betatron amplitude and phase advance, are obtained by means of spectral analysis from the turn-by-turn beam position data. Betatron amplitude measurements lead to poor results, whereas phase advance had a much higher degree of accuracy and stability. The different behavior is probably to be attributed to the intrinsic different nature of the two observables: while phase measurements are essentially time measurements, therefore requiring only a very clean and stable source of clock to provide reliable results, amplitude measurements depend strongly on the calibration accuracy and stability of each one of the four BPM channels, and from the ability of the BPM to give a flat response with respect to a strong change in signal strength due to variations of beam charge.

To improve the quality of the turn-by-turn observations, due care in the tuning of the nonlinear lattice is also needed to avoid fast decoherence phenomena [22]. In fact BPMs are able to sample the betatron motion as long as the particles within each bunch move all together in a coherent oscillation. The ALBA storage ring operates with a vertical unnormalized chromaticity of +4.5. Due to the energy spread, the high value of the chromaticity would wash away the coherent transverse motion in just few hundreds turns, posing a strong restriction on the amount of observable turns, hence limiting the precision of the measurement itself (see Fig. 2, top). In order to avoid the decoherence effects, the vertical chromaticity has been corrected close to zero during the measurements (see Fig. 2, bottom).

Machine stability and fast optics fluctuation also play an important role in turn-by-turn measurements. This is illustrated in Fig. 3, which shows the vertical tune measurements during 100 acquisitions for 120 BPMs. In a single acquisition (zoom in Fig. 3) the tune measurement by 120 BPMs exhibits a standard deviation of $2.1 \times 10^{-6}$, which grows up to $1.1 \times 10^{-4}$ when considering all 100 acquisitions. The cause is likely to be attributed to the noise in the magnet power supplies, which in the case of ALBA is specified to be less than 0.01%. This is in the range of what is expected to produce the observed effect.

### B. Bunch charge and filling patterns

Two different filling patterns are required for the measurement process, one containing only low charge bunches and one containing only high charge bunches. In fact the bunch charge difference between the two filling patterns is one of the key parameters of the measurement and should be maximized as much as possible. We decided to keep the overall amount of charge equal in both configurations, in order to (a) reduce the effects related to the nonperfectly flat response of the BPMs to the beam charge and (b) minimize the heat load effects due to synchrotron radiation. Furthermore, to correctly carry out turn-by-turn measurements some special precaution is needed: the bunches have to be arranged in a short train in order to fit the kicker pulse length and ensure an uniform excitation amplitude along the train itself. While in the low bunch charge case, it is possible to employ a short train where all the buckets are filled with a small amount of charge, the same does not apply for the high charge case where the wakefield interaction can cause instabilities in the trailing bunches and a larger gap between bunches must be used. Figure 4 shows an example of two employed filling patterns: the low charge one made of a train of 45 bunches carrying 0.20 nC on average and the high charge one made of only two

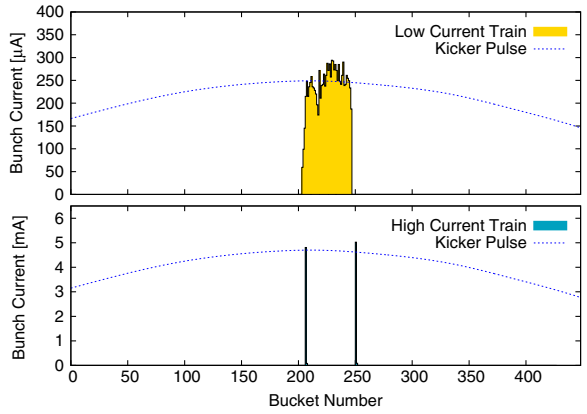


FIG. 4. Two different filling patterns used during the measurements. A low charge per bunch filling pattern (top) composed by a train of 45 buckets, each one filled with 0.20 nC each on average. A high charge filling pattern (bottom) composed by only two bunches carrying around 4.4 nC each. Only the first 50 buckets out of the total 448 are shown. The temporal structure of the magnetic kicker field is also shown, displaying a rather flat profile in the region where the bunches are located.

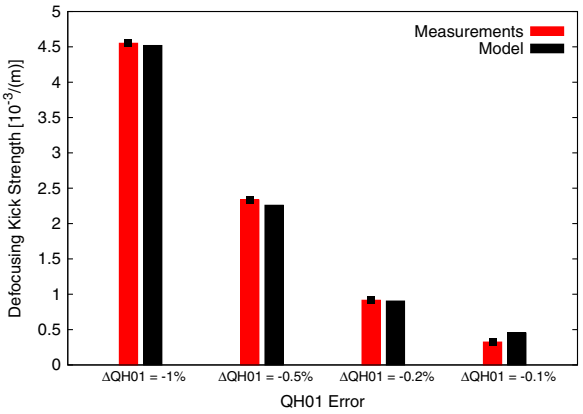


FIG. 5. In red, measured change in the focusing kick for different QH01 setpoints. Each measurement is obtained averaging over data sets containing 100 acquisitions each. The error bars represent the standard deviation of the estimated focusing kick due to the acquisition to acquisition fluctuations. In black, the expected kick based on magnetic calibrations.

bunches of around 4.4 nC each, 90 ns apart. In both cases, the total amount of charge is kept constant to 9 nC.

## IV. MEASUREMENTS RESULTS

### A. Test with a quadrupole error

Before engaging in the proper transverse impedance measurement, a test is carried out by varying a quadrupole setting by a known amount. This provides an easy way to check the functionality of the experimental setup and to directly estimate the amount of noise affecting the measurement.

Given a typical impedance source with a defocusing kick strength $\Delta K$ of 0.1 $(\mathrm{Am})^{-1}$ (Table II), weighted by a bunch charge of 4.4 nC, we calculated an expected defocusing kick of around $5 \times 10^{-4}$ $\mathrm{m}^{-1}$ (that corresponds to 0.1% of the nominal set point of the quadrupole QH01). A defocusing kick of the same magnitude was produced in the storage ring by introducing on purpose a small error in a quadrupole magnet. The measurements collected before and after changing the quadrupole strength where then processed in the same way as in the case of a proper impedance source localized at the quadrupole position.

We chose QH01, which is the quadrupole magnet closest to the injection section, resulting in an effect very similar to the one expected by the transverse impedance of the injection section. We changed the nominal QH01 setting by 1%, 0.5%, 0.2%, and 0.1%, taking 100 acquisitions at each step. The value of QH01 was fitted in order to reproduce the phase beat observed between the measurement at the nominal QH01 setting and each different setting. Figure 5 shows the reconstructed QH01 deviation for each one of the different setpoints, along with the setpoint, showing a very good agreement.

The measurement provides also a simple way to adjust a few parameters, such as the number of acquisitions and the number of turns per acquisition. Already a few hundreds turns were enough to ensure a precision substantially better than the noise due to the fast fluctuations introduced by the residual noise in quadrupoles power supplies. Eventually the number of acquired turns was fixed to 512.

On the other hand, a large number of acquisitions are necessary to counteract the fast fluctuations shown in Fig 3. These optics fluctuations account for most of the noise in the measurements and the only found cure is to average over a large number of acquisitions. Defining the number of acquisitions is a matter of comparing the observed measurement noise from Fig. 5 with the required measurement precision. For each setting of QH01 the measurements have an almost constant statistical error of $\sim 1.1 \times 10^{-4}$ $\mathrm{m}^{-1}$.

In order to explore the main impedance contributors found in Table II, a smaller error would be advisable. Already the injection section, which is one of the most important transverse impedance source, gives a contribution comparable with the measurement error. For this reason we decided to increase from 100 to 500 the number of acquisitions for the impedance measurements, reducing the statistical error by a factor $\sqrt{5}$ with respect to what is observed in Fig. 5. Note that a higher number of acquisitions would lead to other problems, for instance the ability to keep a constant stored current in the ring during the measurements, especially difficult when operating the machine at high charge per bunch and the risk to come across slow thermal drifts. Running the acquisition system at 3 Hz, the whole measurement process lasts less than 3 minutes and causes a stored current drop of less than 5%, which is acceptable for our purposes.

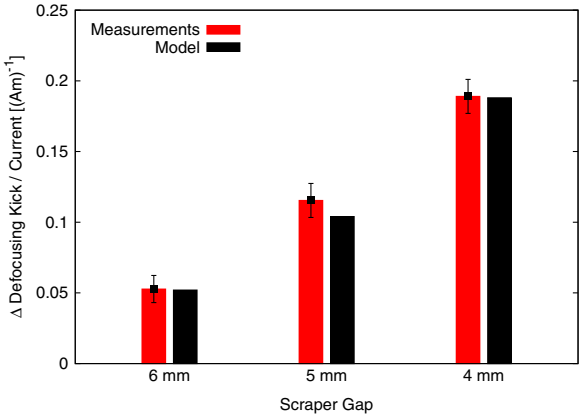


FIG. 6. In red, measured change in the defocusing kick per current unit due to the transverse impedance of the vertical scraper for different gaps with respect to the scraper at nominal position (9.5 mm). Each measurement is obtained averaging over data sets containing 500 acquisitions each. The error bars represent the standard deviation of the estimated focusing kick due to the acquisition to acquisition fluctuations. In black, the predicted values from the impedance computation calculated as kick differences of the considered gap to the nominal scraper gap.

The excellent results validate the ALBA turn-by-turn BPM setup as an effective tool to characterize focusing errors as small as the ones produced by impedance sources. The next step is to test it to evaluate the transverse coupling impedance of a movable scraper.

### B. Test with the vertical scraper

A movable scraper provides a good benchmark to verify the quality of the measurement method by varying a single and well localized impedance source. For this test, only the high charge filling pattern was used and several sets of measurements have been taken for different vertical scraper gaps, each set containing 500 acquisitions. Special attention was paid to keep the stored current decay fairly equal during the acquisitions of all the different data sets, guaranteeing a good cancellation of the contribution due to any other impedance source except the scraper itself.

The measurement with nominal scraper gap (±4.75 mm) was taken as a reference, and its corresponding phase advance was subtracted from the phase advance obtained from each of the other data sets. Then the same fit procedure was used as before to distinguish the vertical defocusing kick produced by the scraper impedance at different gaps. Figure 6 shows the measured defocusing kicks produced by the scraper, following tightly the values provided by the impedance computation for the different configurations. The good agreement brings us to the next step: measuring the absolute contribution of multiple and distributed transverse impedance sources all at once.

### C. Local transverse impedance measurement

Absolute transverse impedance can be measured by repeating a linear optics measurement for different bunch charges. The scraper position was set to the nominal value, while the gap of each IVU was open to the maximum to reduce the impedance contribution to a negligible value. Data were acquired using the high and the low charge filling patterns shown in Fig. 4. Phase beat between high and low charge measurements is extracted (Fig. 7), hereafter the analysis follows the same path as in the previous cases. This time all the elements in Table II (except the IVU) are expected to contribute with a defocusing kick.

Figure 8 shows the result of the analysis including the two strongest impedance sources: the injection section and the beam pipe. The fitting is limited here to these two elements as the effect of the low-gap chambers is actually small due to the rather low beta-function at their location. On the other hand a crosscheck of such assumption is due.

The proof is provided by the measurement of the tune shift $\Delta Q^{\text{meas}}$ induced by the bunch charge, which can be expressed as:

$$\Delta Q^{\text{meas}} = \Delta Q^{\text{fit}} + \Delta Q^{\text{not-fit}} \tag{6}$$

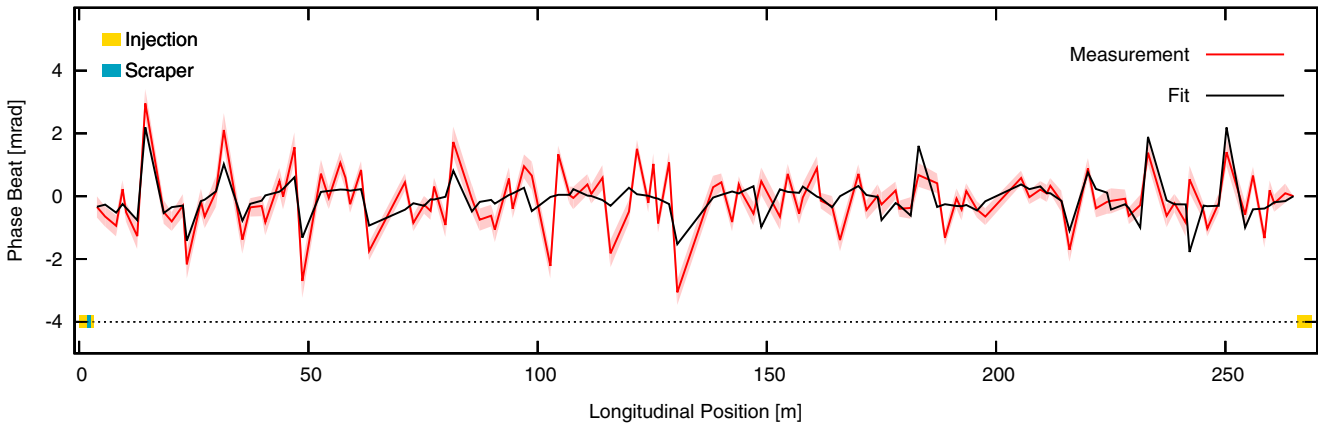


FIG. 7. Measured phase beat for each BPM along with the one computed from the nominal machine model including the two measured defocusing kick produced by the beam pipe and the injection section.

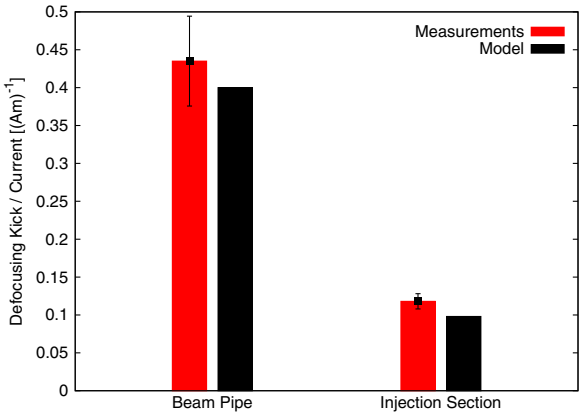


FIG. 8. In red, the defocusing kick strength per current unit obtained from the fit including the beam pipe and the injection section. Each measurement is obtained averaging over data sets containing 500 acquisitions each. The error bars represent the standard deviation of the estimated focusing kick due to the acquisition to acquisition fluctuations. In black, the predicted value from the impedance computation.

where $\Delta Q^{\text{fit}}$ corresponds to the tune shift induced by the two fitted impedance sources (beam pipe and injection section) and $\Delta Q^{\text{not-fit}}$ is the tune shift produced by all the impedance sources not accounted by the fit.

A satisfactory agreement was found, as the tune measurement revealed a tune shift $\Delta Q^{\text{meas}} = -2.3 \times 10^{-3}$ where a value $\Delta Q^{\text{fit}} = -1.8 \times 10^{-3}$ was inferred from the two fitted impedance sources, leading to a discrepancy of around 22%, confirming that most of the coupling contributors have been correctly taken into account by the impedance model.

The discrepancy between the left- and right-hand side of Eq. (6) gets smaller if we consider also the impedance sources that have not been included in the fit that all together provide still a not completely negligible contribution. Adding up the tune shift induced by all the elements presented in Table II except for the IVUs, which where opened to the maximum gap, the beam pipe and the injection section, already considered by the fit, we obtain an overall tune shift $\Delta Q^{\text{not-fit}} = -0.46 \times 10^{-3}$, reducing the discrepancy to 2%.

The agreement between the measurements and the values obtained by the impedance computation confirms that the machine impedance model is sound and well understood (see Ref. [23]). In particular, it could be shown that the actual impedance model of the Ti-coated ceramic chambers of which 4 are located in the injection section is about correct.

### D. Impedance of an in-vacuum undulator

The vertical impedance kicks provided by the low-gap chambers and IVUs are *a priori* stronger than by other vacuum chamber contributions, in fact the small values of the vertical betatron function of the ALBA nominal lattice at their position distinctly mitigate their effect [Eq. (3)].

To gain sensitivity, the nominal lattice has been detuned at the location of one of the IVU increasing the vertical beta function by a factor 5.2 (see Fig. 10 and Ref. [24]), resulting in an increase of the phase beating due to the defocusing kick induced by the impedance.

Repeating the same measurements of the phase beat as in Sec. IV C (Fig. 9), but in this case using the lattice with high vertical beta at the IVU, allows us to characterize its impedance. The gap of the insertion device was closed to 6 mm, and the same procedure used in the previous case was repeated. Figure 11 shows the results of the analysis including the defocusing kick produced by the insertion device impedance along with the one of the injection section and the beam pipe. The measurement results for the injection section and for the beam pipe are consistent with the previous analysis, while the effect of the insertion device is estimated with an even smaller statistical error, that makes the 20% discrepancy respect to the theoretical predictions not negligible. On the other hand the phase beat fit (Fig. 9) shows a rather good agreement confirming the reliability of the measurement.

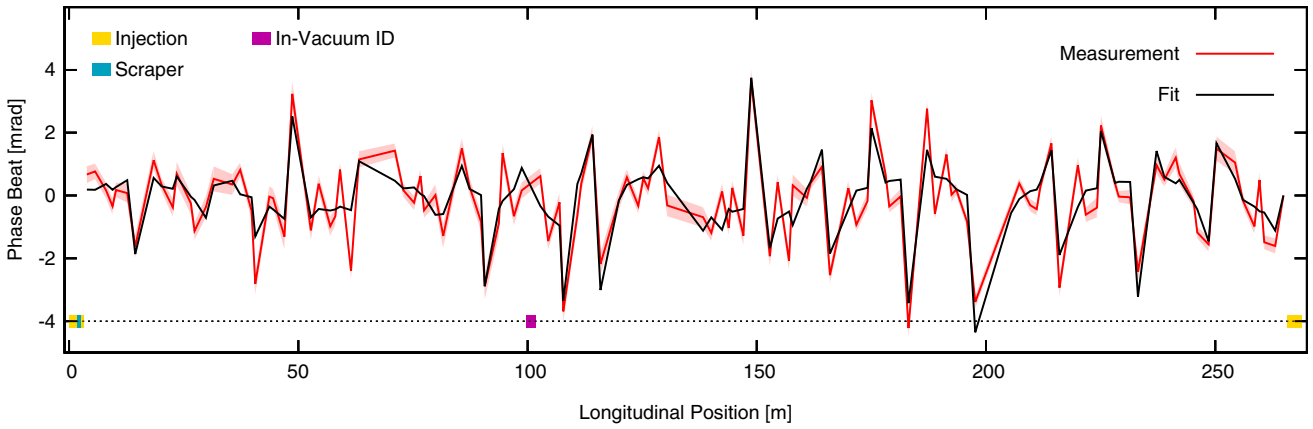


FIG. 9. Measured phase beat for each BPM along with the one computed from the high $\beta_v$ model including the three measured defocusing kicks produced by the beam pipe, the injection section and the IVU located at the high vertical beta position.

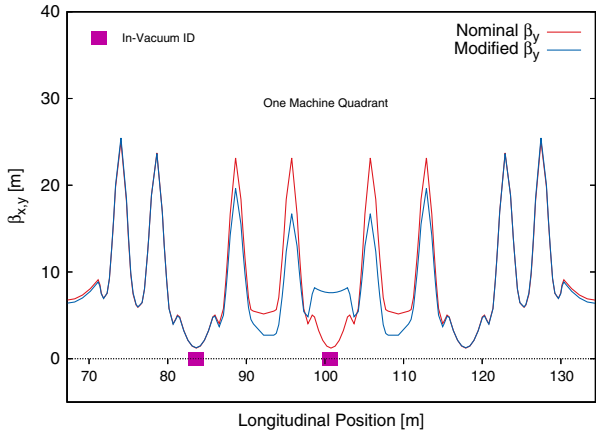


FIG. 10. Vertical betatron functions for the nominal and modified ALBA lattices. The average vertical betatron function has been increased from 1.2 m to 6.5 m at the location of one IVU.

Since measurements and computations are supposed to be affected by very different error sources, the observed discrepancy allows us to set a limit on the overall measurement uncertainty, including all the systematic errors that would be barely estimated otherwise. The most significant disagreement between measurement and simulation is found in the case of the IVU, exhibiting an overall kick discrepancy of $\sigma_K = 0.029\ (\mathrm{Am})^{-1}$ equivalent to a transverse impedance of 7.6 $\mathrm{k\Omega/m}$ (20% of the model value of 38.2 $\mathrm{k\Omega/m}$). On the other hand, since the phase beat induced by an impedance source is proportional to the beta value, a better error estimation is obtained by multiplying the kick error by the beta, $\beta\sigma_K = 0.19\ \mathrm{A}^{-1}$ equivalent to a $\beta$-weighted transverse impedance of 49 kΩ.

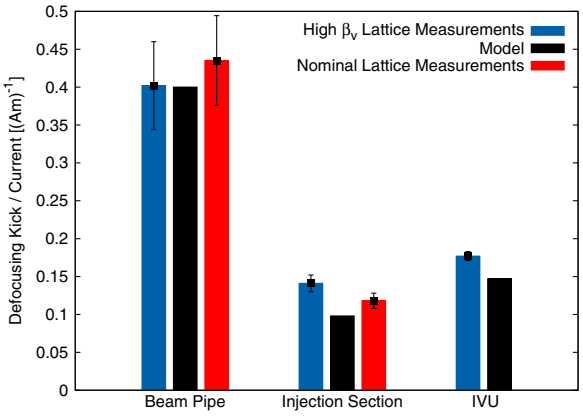


FIG. 11. In blue the defocusing kick strength per current unit obtained from the fit including the beam pipe, the injection section and the IVU located at the high vertical beta spot. Each measurement is obtained averaging over data sets containing 500 acquisitions each. The error bars represent the standard deviation of the estimated focusing kick due to the acquisition to acquisition fluctuations. In black is the predicted value from the impedance computation while red bars represent the defocusing kick obtained from the previous measurement (Fig. 8) where the nominal lattice was employed.

## V. MEASUREMENT LIMITS AND POSSIBLE IMPROVEMENTS

In order to characterize smaller impedance contributors an improved sensibility and a reduction of noise and systematic errors is desirable. In this section we propose a few options to improve the overall measurements quality, which for technical limitations of the present ALBA experimental setup could not be tested. Nevertheless we think that it would be beneficial for machines equipped with more advanced hardware [25,26].

Two main factors were identified as the main source of measurement uncertainty: fast optics fluctuations, due to the electric noise in the quadrupoles power supplies (see Fig. 3); and slow machine drifts, likely due to the different thermal loads on the machine components produced by the different filling patterns.

Having identified the main sources of error, we can proceed to analyze possible solutions. Regarding machine drifts related with filling pattern, a possible cure is found by storing at the same time a high and a low current bunch trains in a hybrid filling pattern fashion. In this configuration there is no need anymore to switch from one filling pattern to the other, avoiding thus different thermal loads in the machine. Moreover, avoiding the injection of a different filling pattern between acquisitions results in the beneficial side effect of speeding up the measurement process, reducing also the effect produced by any other slow machine drift unrelated with the change in filling pattern. To discriminate the signal produced by only one of the two trains, BPMs with sub-turn resolution are needed. Unluckily the radio-frequency front-end employed in the BPM system of ALBA does not meet such requirements, preventing us from testing this option.

Since the employed BPM system does not provide any way to isolate the signal produced by each one of the two trains, a way to disentangle the two signals downstream is required. An option is provided by the small tune shift due to the optic distortion itself produced by the transverse impedance. In this case the two signals are acquired simultaneously and separated afterwards by means of spectral analysis. In this approach BPMs with sub-turn resolution are not required, instead very good linearity is mandatory. A first attempt to apply the proposed techniques at ALBA did not deliver the expected results, more tests are currently being carried out.

## VI. CONCLUSION

Using BPM turn-by-turn data, we succeeded in measuring the individual defocusing effects produced by different transverse impedance sources of the ALBA storage ring, including elements like scraper, injection zone, in-vacuum

undulator and standard vacuum beam pipe. The satisfactory agreement between the measurements and the transverse impedance model based on analytical calculation of the resistive wall and GdfidL simulation of the geometrical impedance confirmed that the turn-by-turn technique is a valid diagnostic tool to carry out very sensitive and non-intrusive optics measurements.

Furthermore it has been shown how the smaller impedance sources can still be properly characterized by manipulating the machine optics in order to obtain a magnification of the induced defocusing kick. This method has been used to characterize the impedance of one of ALBA's IVU. The measurement differs only by about 20% of the value given by the transverse impedance model. The required complexity arising from the change of the machine optics limited the test of such approach only to this particular IVU, but it could be applied to any other insertion device.

The magnet power supplies noise has been identified as one of the main limitation for a fast optics measurement. In fact the continuous machine optics fluctuations forced us to extend the measurement over a period longer than otherwise required, in order to average out the noise. The extended measurement time runs against other requirements such as the ability to maintain a constant stored current and definitely making the measurement more prone to machine drifts. A solution to overcome such limitation has been proposed. Unfortunately because of technical limitations in the ALBA BPM system we cannot check it out, whereas newer machines employing the very last generation BPMs [25,26] could benefit from such refined approach.

## ACKNOWLEDGMENTS

The authors would like to acknowledge the support of J. Moldes, A. Olmos, and the ALBA operations group.

[1] A. W. Chao, *Physics of Collective Beam Instabilities in High Energy Accelerators* (Wiley, New York, 1993).

[2] D. Brandt, P. Castro, K. Cornelis, A. Hofmann, G. Morpurgo, G. L. Sabbi, J. Wenninger, and B. Zotter, Conference Proceedings **C950501**, 570 (1996).

[3] R. T. Dowd, M. J. Boland, G. LeBlanc, M. J. Spencer, and Y. E. Tan, Single Bunch Studies at the Australian Synchrotron, in *Proceedings, European Particle Accelerator Conference, EPAC08* (2008), p. TUPC010, https://cds.cern.ch/record/1183159.

[4] A. S. Muller, I. Birkel, E. Huttel, F. Perez, M. Pont, and F. Zimmermann, in *Proceedings of the 9th European Particle Accelerator Conference, Lucerne, 2004* (EPS-AG, Lucerne, 2004) http://accelconf.web.cern.ch/AccelConf/e04/.

[5] H. Burkhardt, G. Rumolo, and F. Zimmermann, in *Proceedings of the 8th European Particle Accelerator Conference, Paris, 2002* (EPS-IGA and CERN, Geneva, 2002), p. 1449.

[6] T. Günzel, U. Iriso, F. Pérez, E. Koukovini-Platia, and G. Rumolo, Analysis of Single Bunch Measurements at the ALBA Storage Ring, in *Proceedings, 5th International Particle Accelerator Conference (IPAC 2014), Dresden, Germany* (2014), p. TUPRI052, http://jacow.org/IPAC2014/papers/tupri052.pdf.

[7] U. Iriso, H. Bartosik, T. Günzel, E. Koukovini-Platia, and G. Rumolo, Beam-based Impedance Characterization of the ALBA Pinger Magnet, in *Proceedings, 6th International Particle Accelerator Conference (IPAC 2015)* (Richmond, Virginia, 2015), p. MOPJE027, http://accelconf.web.cern.ch/AccelConf/IPAC2015/papers/mopje027.pdf.

[8] V. Sajaev, in *Proceedings of the 2003 Particle Accelerator Conference, Portland, OR* (IEEE, New York, 2003), Vol. 1, p. 417, ISSN .

[9] V. Smaluk, R. Fielder, A. Blednykh, G. Rehm, and R. Bartolini, Phys. Rev. ST Accel. Beams **17**, 074402 (2014).

[10] G. Arduini, C. Carli, and F. Zimmermann, in *Proceedings of the 9th European Particle Accelerator Conference, Lucerne, 2004* (EPS-AG, Lucerne, 2004), http://accelconf.web.cern.ch/AccelConf/e04/.

[11] R. Calaga, G. Arduini, E. Métral, G. Papotti, D. Quatraro, G. Rumolo, B. Salvant, and R. Tomás, in *Proceedings of the 23rd Particle Accelerator Conference, Vancouver, Canada, 2009* (IEEE, Piscataway, NJ, 2009), p. FR5RFP034.

[12] N. Biancacci, M. Blaskiewicz, Y. Dutheil, C. Liu, K. Mernick, M. Minty, and S. White, Transverse Impedance Measurement in RHIC and the AGS, in *Proceedings, 5th International Particle Accelerator Conference (IPAC 2014)* (Dresden, Germany, 2014), p. TUPRI071, http://jacow.org/IPAC2014/papers/tupri071.pdf.

[13] N. Biancacci and R. Tomás, Phys. Rev. Accel. Beams **19**, 054001 (2016).

[14] N. Biancacci, Ph.D. thesis, Università degli Studi di Roma "La Sapienza", 2014.

[15] R. Nunez, M. Pont, and E. Huttel, Conference Proceedings **C110904**, 2421 (2011).

[16] www.gdfidl.de.

[17] M. Pont, N. Ayala, G. Benedetti, M. Carlà, Z. Martí, and R. Núnez-Prieto, A Pinger Magnet System for the ALBA Synchrotron Light Source, in *Proceedings, 6th International Particle Accelerator Conference (IPAC 2015)* (Richmond, Virginia, 2015), p. WEPMN050, http://accelconf.web.cern.ch/AccelConf/IPAC2015/papers/wepmn050.pdf.

[18] http://www.i-tech.si.

[19] M. Carl, G. Benedetti, Z. Martí, and L. Nadolski, Optimization of Turn-by-Turn Measurements at Soleil and Alba Light Sources, in *Proceedings, 6th International Particle Accelerator Conference (IPAC 2015)* (2015), p. TUPJE035, http://accelconf.web.cern.ch/AccelConf/IPAC2015/papers/tupje035.pdf.

[20] K. Scheidt, Modified (adjustable) ddc filters within libera brilliance—experience with partial fill patterns and pure t-b-t measurements, http://www.i-tech.si/file/download/197_95d54d88347c/stat.

[21] A. Kosicek, V. Poucki, T. Karcnik, and B. K. Scheidt, Modified Digital Filtering Makes Possible "True & Pure" t-b-t Measurements, in *Proceedings of BIW08, Lake Tahoe* (California, 2008).

[22] A. Franchi, L. Farvacque, F. Ewald, G. Le Bec, and K. B. Scheidt, Phys. Rev. ST Accel. Beams **17**, 074001 (2014).

[23] T. Günzel and U. Iriso, Revision of the Impedance Model for the Interpretation of the Single Bunch Measurements at ALBA, in *Proceedings, 6th International Particle Accelerator Conference (IPAC 2015)* (2015), p. MOPJE026, http://accelconf.web.cern.ch/AccelConf/IPAC2015/papers/mopje026.pdf.

[24] Z. M. G. Benedetti and J. Campmany, Low Horizontal Beta Optics for ALBA, in *Proceedings of IPAC2016, Busan, Korea* (2016), p. THPMR035.

[25] B. Podobedov, Single Micron Single-bunch Turn-by-turn BPM Resolution Achieved at NSLS-II, in *Proceedings of IPAC2016, Busan, Korea* (2016).

[26] http://www.ohwr.org/projects/bpm/wiki.